Extracellular ATP activates the NLRP3 inflammasome and is an early danger signal of skin allograft rejection

Joaquín Amores-Iniesta[1†], Maria Barberà-Cremades[1†], Carlos M. Martínez[1], José A. Pons[1], Beatriz Revilla-Nuin[1], Laura Martínez-Alarcón[1], Francesco Di Virgilio[2], Pascual Parrilla[1], Alberto Baroja-Mazo[1], Pablo Pelegrín[1*]

[1]Experimental Surgery Group, [2]Experimental Pathology Unit, Biomedical Research Institute of Murcia (IMIB-Arrixaca), University Clinical Hospital Virgen de la Arrixaca, 30120 Murcia, Spain
[3]Department of Morphology, Surgery and Experimental Medicine, University of Ferrara, 44121 Ferrara, Italy

*Lead contact/corresponding author: Dr. Pablo Pelegrín, Edificio LAIB 4ª planta, Instituto Murciano de Investigación Biosanitaria (IMIB-Arrixaca). Carretera Buenavista. 30120 Murcia, Spain. Phone: +34 868885038; e-mail: pablo.pelegrin@imib.es

†These authors contributed equally

RUNNING TITTLE: ATP release in allotransplantation

KEYWORDS: allotransplantation, caspase-1, IL-18, macrophages, NLRP3 inflammasome, P2X7 receptor

COMPETING FINANCIAL INTERESTS:
The authors declare no competing financial interests.

SUMMARY

Immune cells are equipped with a number of receptors that recognize sterile injury and pathogens. We find that host immune cells release ATP as an inflammatory signal in response to allogeneic transplantation. ATP then acts via a feedback mechanism on the P2X7 channel to activate the NLRP3 inflammasome and subsequently process and release interleukin (IL)-18. This process is a necessary stage in the deleterious Th1 response against allotransplantation via interferon-γ production. Lack of IL-18 resulted in a decrease in graft-infiltrated CD8 cells, but an increase in regulatory T cells. In human liver transplant patients subjected to progressive immunosuppressive drug withdrawal, we found that patients suffering acute rejection had higher levels of the P2X7 receptor in circulating inflammatory monocytes compared to tolerant patients. These data suggest that the pharmacological inhibition of the P2X7 receptor or the NLRP3 inflammasome will aid in inducing transplant tolerance without complete immunoparalysis.

INTRODUCTION

Transplantation of antigen-containing tissues between non-genetically identical individuals is referred to as allogenic organ transplantation. This procedure is growing in popularity with over 38,000 procedures occurring in 2016 in the USA alone (Bentley and Phillips, 2017). However, in allogeneic organ transplantation, antigens in graft tissues can lead to non-self-recognition and thus generate a destructive immune response in the form of tissue rejection. Nevertheless, non-infected transplants are sterile and are beneficial rather than dangerous to the recipient organism (Land, 2012). The allogeneic immune response is initiated when innate antigen-presenting cells present non-self antigens to lymphocytes, resulting in a destructive adaptive Th1 response to grafts. Tissue damage caused by the transplantation procedure results in the release of damage-associated molecular patterns (DAMPs) which activate innate immunity during allograft rejection. These DAMPs include the induction of heat shock proteins, the production of reactive oxygen species, hypoxia and the degradation of the extracellular matrix (Critchley and Fildes, 2012; Land, 2012; Matzinger, 2002). Recently it has also been demonstrated that innate antigen-presenting cells recognize and are directly activated by alloantigens (Oberbarnscheidt et al., 2014; Zecher et al., 2009). However, the way that endogenous DAMPs are regulated and elicit an allogeneic immune response is poorly understood.

The pro-inflammatory cytokine interleukin (IL)-1β plays a key role in host responses to infection and tissue injury. IL-1β is expressed in an inactive pro-form which is cleaved into an active form by the protease caspase-1 (Cassel and Sutterwala, 2010). Activation of caspase-1 is regulated by a group of large multi-protein complexes referred to as inflammasomes formed by cytosolic pattern recognition receptors (PRRs), often of the nucleotide-binding domain and leucine-rich repeat containing receptor (NLR) family. The best characterized inflammasome is NLRP3 (Cassel and Sutterwala, 2010). Inflammasomes are composed of the PRR and pro-caspase-1 and, in some types, the adaptor apoptosis-associated speck-like protein containing a caspase recruitment domain (ASC) that interacts via homology, thus binding domains with the PRR and pro-caspase-1 (Latz et al., 2013). Activating NLRP3 inflammasome requires a priming signal to increase the expression of the receptor and of pro-IL-1β and a second signal (i.e. the activation of the P2X7 receptor by extracellular ATP) to induce inflammasome formation, activate caspase-1 and process pro-IL-1β into a mature cytokine that is secreted from the cell via unconventional protein release mechanisms (Cassel and Sutterwala, 2010; Latz et al., 2013). Extracellular ATP is a key DAMP that induces NLRP3 inflammasome formation by signaling through the purinergic P2X7 cell surface receptor (Di Virgilio et al., 2017; Ferrari et al., 2006; Idzko et al., 2014). The P2X7 receptor is associated with two different membrane permeabilities: 1) a fast cation conductance that increases cytosolic Ca^{2+} and decreases intracellular K^{+}, these being key triggers of NLRP3 inflammasome activation; and 2) a second permeability after prolonged ATP stimulation that allows the passage of molecules of up to ~900 Da in molecular weight (Pelegrin, 2011a). NLRP3 and the subsequent caspase-1 activation also regulate the release of IL-18, another

pro-inflammatory cytokine that is a potent inducer of the Th1 response because it produces interferon (IFN)-γ (Novick et al., 2013). The IL-18 precursor is constitutively expressed in cells and does not require gene induction (Novick et al., 2013); this difference in expression when compared to IL-1β is critical in conditions where there is no priming signal and, therefore, no pro-IL-1β. A clear example of this can be seen in the autoinflammatory syndromes caused by mutations in NLRP3 where systemically elevated levels of IL-18 are present but IL-1β is not usually detectable (Baroja-Mazo et al., 2014; Novick et al., 2013). Therefore, IL-1β and IL-18 will affect pathogenesis differently depending on the nature of the disease or injury. Allotransplantation rejection involves a substantial innate and adaptive immune response in which the roles of IL-1β and IL-18, their upstream regulators NLRP3, caspase-1 and extracellular ATP and the P2X7 receptor have yet to be fully understood.

In this study, we found that the innate immune system is activated by extracellular ATP during allotransplantation. We observed that soon after allogeneic (but not syngeneic) transplantation, antigen-presenting cells modulated extracellular ATP independently of cell death and via a mechanism involving the P2X7 receptor. This signaling activates the NLRP3 inflammasome and releases IL-18 to ensure allograft rejection. We demonstrate that pharmacological blockage of the P2X7 receptor decreases the concentration of extracellular ATP and increases graft survival and that this could represent a new procedure for developing graft tolerance without complete immunosuppression. Our work also raises clinical awareness of the need to correctly manage DAMPs in transplantation medicine.

RESULTS

Increased extracellular ATP in allogeneic transplantation

Using the pmeLuc biosensor (Pellegatti et al., 2005) we found that at 3 days after conducting separate allogeneic and syngeneic skin transplants in mice, extracellular ATP was higher in the allogeneic transplants and was locally associated with the grafted allogeneic skin (**Figure 1A,B**). We confirmed that in the control group at 14 days post-transplantation, allogeneic tissue was rejected whereas syngeneic tissue was tolerated (**Figure S1A**). Degradation of extracellular ATP by local injection of exogenous apyrase reduced the bioluminescence signal in allografts but did not significantly decrease the bioluminescence signal from an intracellular luciferase reporter assay (**Figure S1B,C**), thus confirming that the bioluminescence signal of pmeLuc was due to extracellular ATP. Extracellular ATP is considered a tissue-damage-associated molecule (Idzko et al., 2014) and could be passively released from cells during the process of allogeneic tissue destruction (Oberbarnscheidt and Lakkis, 2014). However, we found that while extracellular ATP decreased over time after allogeneic tissue transplantation (**Figure 1C**), allogeneic tissue damage actually increased (**Figure 1D**). Therefore, elevated extracellular ATP in the early stages of allotransplantation cannot be considered a direct consequence of surgery, the allogeneic immune response, or the associated tissue damage. Despite elevated local extracellular ATP 3 days after allotransplantation (**Figure 1C**), the allogeneic-associated adaptive immune response was not observed until day 7, when we found an increase in infiltrating CD3-lymphocytes and a robust production of the IFN-γ and IL-12 cytokines (**Figure 1E-G** and **Figure S1D**). This late adaptive immune response is expected in skin transplants that are not immediately vascularized. This is in contrast to rapidly vascularized grafts where T cells infiltrate the graft within hours and produce IFN-γ (Su et al., 2014). The slower adaptive response in the skin model suggests that extracellular ATP is produced as an early inflammatory signal in allografts before the Th1 allogeneic immune response is generated.

The P2X7 receptor modulates ATP release in allografts

Extracellular ATP is a danger signal that triggers macrophage NLRP3 inflammasome by activating the purinergic P2X7 receptor (Idzko et al., 2014; Pelegrin, 2011b; Schroder and Tschopp, 2010). Consequently, we used a genetic approach to study the ATP release mechanism in allografts. We found that ATP release was absent in *P2xr7*$^{-/-}$ mice 3 days after allotransplantation (**Figure 2A**), suggesting that the P2X7 receptor modulates the extracellular levels of its own agonist *in vivo*. This was also confirmed when wild-type mice were treated with the selective P2X7 receptor antagonist A438079 (Donnelly-Roberts and Jarvis, 2007); the wild-type mice showed a significantly lower extracellular ATP response to allogeneic grafts than vehicle treated mice (**Figure 2B**). We next found that the P2X7 receptor was mainly expressed to roughly the same levels by macrophages in both syngeneic and allogeneic grafts (**Figure S2A-C**). The decrease in extracellular ATP found at 3 days

post-transplantation in *P2xr7*$^{-/-}$ mice was not due to a decrease in the amount of graft-infiltrating macrophages (**Figure S2D**). Extracellular ATP increased in supernatants from macrophages incubated *in vitro* with allogeneic, but not syngeneic, skin tissue (**Figure 2C**), and after incubation with the classic antigen ovalbumin (**Figure 2D**). Ovalbumin was able to induce ATP release via the P2X7 receptor (**Figure 2D**) and increase early macrophage plasma membrane permeabilization after activation of the P2X7 receptor (**Figure 2E**). This suggests that the P2X7 receptor-associated pore could be a pathway for ATP release during antigen processing by macrophages (Pelegrin, 2011a). We next investigated the role of the macrophage P2X7 receptor in the release of ATP during allogeneic transplantation by supplementing allografts on *P2xr7*$^{-/-}$ mice with wild-type or *P2xr7*$^{-/-}$ macrophages. *In vivo* supplementation of wild-type macrophages in the *P2xr7*$^{-/-}$ host restored local extracellular ATP to about the same level seen in wild-type mice (**Figure 2F**). Conversely, allogeneic transplantation of P2X7-deficient skin onto wild-type recipients presented a similar level of extracellular ATP when compared to wild-type skin (**Figure S2E**). This suggests that allograft recognition *in vivo* by recipient macrophages amplifies the release of ATP via the P2X7 receptor and that donor immune cells do not release extracellular ATP in the skin transplantation model.

Blocking the P2X7 receptor reduces allograft rejection

We next found lower levels of epithelial hyperplasia in the transplanted skin of *P2xr7*$^{-/-}$ mice after 3 days (**Figure 3A,B**). Epithelial hyperplasia is an early sign of skin distress (Lee et al., 2009) and we observed low levels of hyperplasia in syngeneic grafted mice compared to the extensive levels in allogeneic grafted mice (**Figure 3A,B** and **Figure S3A,B**). Furthermore, treatment of wild-type allotransplanted animals with A438079 also resulted in decreased epithelial thickness (**Figure 3B** and **Figure S3A**), thus demonstrating the therapeutic potential of reducing extracellular ATP by early targeting of the P2X7 receptor during the period immediately after the transplant procedure. Furthermore, in terms of the Banff pathological classification for skin allografts (Cendales et al., 2008), rejection severity was lower at 7 days after transplantation in *P2xr7*$^{-/-}$ mice (Banff score 3) compared to wild-type animals (Banff score 4). *P2xr7*$^{-/-}$ mice or mice treated with A438079 also presented decreased inflammatory infiltrate, reduced necrosis and preserved epidermal and dermal allograft structure at 7 days after transplantation (**Figure 3A** and **Figure S3A**). *P2xr7*$^{-/-}$ mice presented reduced levels of specific allogeneic IgGs in serum at 14 days after transplantation (**Figure S3C**), suggesting that the P2X7 receptor is important in establishing a full allogeneic response driven by B cells. This was paralleled by a decrease in allograft-infiltrating $CD3^+$ T cells and $F4/80^+$ macrophages at 7 days after transplantation in *P2xr7*$^{-/-}$ mice (**Figure 3C** and **Figure S3D**). In addition, allotransplanted mice treated with A438079 showed lower IFN-γ concentrations in serum when compared to allotransplanted wild-type mice (**Figure 3D**). This was matched by a reduction in IFN-γ production after the expansion of T cells in response to BALB/c alloantigens (**Figure 3E**), thus suggesting that blocking the P2X7 receptor's activation and

extracellular ATP causes defective T cell activation in allotransplants. This reduced alloimmune response increased the survival rates of allogeneic transplanted tissues (**Figure 3F,G** and **Figure S3E**). Overall, we have shown that transplantation of allogeneic, but not syngeneic, tissue induces an early release of ATP from innate immune cells via the P2X7 receptor and thus establishes an efficient alloimmune response driven by the T and B cells.

P2X7 receptor expression increases during human liver allograft rejection

To obtain evidence of the potential importance of the P2X7 receptor during human transplant rejection, we analyzed the expression of the P2X7 receptor on the surface of inflammatory blood monocytes ($CD14^{+}CD16^{++}$) in liver transplant patients after controlled immunosuppression withdrawal. Some patients rejected the transplant during immunosuppression withdrawal (non-tolerant patients), while other patients became tolerant to it (tolerant patients) (**Table S1**). After immunosuppression withdrawal, plasma concentration of liver enzymes increased during acute rejection in non-tolerant patients when compared to tolerant patients (**Figure 3H** and **Figure S4A**). Liver biopsy corroborated immune rejection of the liver in patients with increased levels of liver enzymes in plasma (not shown). During rejection, P2X7 receptor expression in circulating inflammatory monocytes increased (**Figure 3H**) without changing the percentage of inflammatory monocytes (**Figure S4B**). In tolerant patients, P2X7 receptor expression was similar both during immunosuppression and after withdrawal (**Figure 3H**). The fold change of plasma ATP concentration measured during immunosuppression and after rejection in non-tolerant patients positively correlated with the fold change in plasma liver enzymes (**Figure 3I**), suggesting that extracellular ATP and the P2X7 receptor could play a role in the immune allogeneic response during rejection of liver transplants in humans.

The P2X7 receptor engages the NLRP3 inflammasome in allografts

We next analyzed whether P2X7 receptor-induced pyroptosis could be the mechanism for ATP release in allografts, given that the P2X7 receptor is a well-known activator of caspase-1 via the canonical NLRP3 inflammasome pathway and that caspase-1 is involved in pyroptosis, a specific type of cell death characterized by the release of intracellular components (Miao et al., 2011). However, we did not find any difference in extracellular ATP levels in allografts from wild-type versus *Nlrp3*$^{-/-}$ or *Casp1/11*$^{-/-}$ mice (**Figure 4A,B**). These data suggest that upon alloantigen recognition, pyroptosis mediated by activation of either caspase-1 or caspase-11 does not induce ATP release, but rather that the P2X7 receptor in macrophages induces a pathway for ATP release (Pellegatti et al., 2005), which in turn could feed back into the P2X7 receptor itself. It is well known that the P2X7 receptor activates the NLRP3 inflammasome, this being a key event in the activation of the adaptive immune system (Pelegrin, 2011b; Schroder and Tschopp, 2010). We found that *Casp1* and *Il1b* gene expression was upregulated in allografts at 3 days post-transplantation and that this upregulation was reduced by A438079 treatment (**Figure 4C**). *Nlrp3* gene expression was

also upregulated at 3 days post-transplantation to the same extent in both syngeneic and allogeneic transplants (**Figure 4C**). This suggests that *Nlrp3* expression might be caused by tissue damage during surgery, as has been demonstrated in a sterile injury model (Komada et al., 2015). We also found constitutive expression of the *Il18* gene in both syngeneic and allogeneic grafts (**Figure 4C**), in line with the fact that IL-18 is expressed as a constitutive gene with its release controlled by the activation of caspase-1 (Novick et al., 2013). However, the circulating blood concentration of IL-18 increased in allotransplanted mice after 3 days and reduced in allotransplanted mice treated with A438079 (**Figure 4D**). Despite increased local *Il1b* gene expression in the allografts (**Figure 4C**), this cytokine was not identified at systemic level in the serum at days 3 or 7 post-transplantation. This indicates that the P2X7 receptor could regulate the NLRP3-inflammasome at an early stage after allotransplantation to induce systemic IL-18 cytokine *in vivo*.

NLRP3 inflammasome signaling contributes to the severity of allograft rejection

Several inflammasome related genes were further upregulated in allografts at day 7 post-transplantation (**Figure 5A-C**). Upregulation of *Casp1* gene expression in allografts was reduced in *Nlrp3*$^{-/-}$ mice (**Figure 5A**), while *Nlrp3* and *Il1b* upregulation were significantly decreased in *Casp1/11*$^{-/-}$ mice (**Figure 5B,C**). These data show that early induction of the inflammasome by P2X7 receptor signaling is persistent (up to at least 7 days after allogeneic transplantation) via a positive feedback loop induced by the NLRP3-inflammasome itself. We next found that NLRP3-inflammasome deficiency reduced epithelial hyperplasia after 3 days (**Figure 6A,B** and **Figure S5A**). Histological tissue damage observed 7 days after transplantation was less severe in allotransplanted *Nlrp3*$^{-/-}$ and *Casp1/11*$^{-/-}$ mice than in allotransplanted wild-type mice (**Figure 6A** and **Figure S5B**). Furthermore, when compared to wild-type mice, *Nlrp3*$^{-/-}$ and *Casp1/11*$^{-/-}$ allotransplanted mice presented significantly reduced circulating IL-18 cytokine (**Figure 6C**) and a decreased number of allograft infiltrating CD3^{+} T cells and F4/80^{+} macrophages (**Figure 6D** and **Figure S5C,D**). In addition, 7 days after transplantation, allotransplanted *Nlrp3*$^{-/-}$ and *Casp1/11*$^{-/-}$ mice showed low *Ifng* gene expression in the allograft and lower IFN-γ serum concentration when compared to allotransplanted wild-type mice (**Figure 6E,F**). This was paralleled by reduced IFN-γ production when T cells expanded in response to BALB/c alloantigens in mixed leukocyte reactions (**Figure 6G**), thus suggesting that a lack of NLRP3 inflammasome causes defective T cell activation in allotransplants.

IL-18 mediates allograft rejection

To determine whether the increase in IL-18 could be mediating the allograft rejection response, we first measured the IL-18 binding protein (IL-18BP) in the serum of transplanted animals to verify that enough free IL-18 was available for signaling. Allogeneic transplantation did not increase IL-18BP concentration, and the levels of free IL-18 were significantly higher for allogeneic transplantation when compared to syngeneic transplantation (**Figure 7A**). We

found that IL-18 was not detectable in the serum of IL-18 knock-out mice (**Figure S6A**) and that their concentrations of IL-18BP were not affected (**Figure S6A**). However, the amounts of IL-12p40 and IFN-γ were significantly reduced in IL-18 deficient mice when compared to wild-type animals (**Figure 7B,C**). Furthermore, a mixed lymphocyte reaction produced less IFN-γ when the lymphocytes derived from the allogeneic transplanted IL-18 knock-out mice (**Figure 7D**). The amount of IL-12p40 and IFN-γ was not reduced in IL-1 receptor 1 deficient mice (**Figure S6B,C**), suggesting that IL-18 (and not IL-1β) plays a role in the inflammasome-mediated allogeneic response. This was further confirmed by histology 7 days after allotransplantation. IL-18 deficient mice showed a conserved dermis and cutaneous gland structure (**Figure 7E**), with a calculated Banff score of 2 compared to a score of 4 in wild type mice. However, IL-1R1 deficiency resulted in destruction and necrosis of the dermis and epidermis (**Figure S6D**). Although macrophages in the allogeneic transplant were lower in IL-18 deficient mice than in wild-type mice, $CD3^+$ lymphocyte cell infiltration was similar in both types of mice (**Figure 7F**). However, the number of $CD8^+$ lymphocytes was significant lower in IL-18 knock-out mice than in wild-type or IL-1R1 deficient mice (**Figure 7F** and **S6E,F**), and IL-18 deficient mice showed an increase in T-regulatory cells (**Figure 7F** and **S6G**). Overall, we show that transplantation of allogeneic, but not syngeneic, tissue induces an early release of ATP from innate immune cells via the P2X7 receptor, which engages the NLRP3 inflammasome and establishes a detrimental alloimmune response via IL-18 signaling.

DISCUSSION

Organ transplantation is a sterile situation where a destructive immune response is developed due to non-self-antigen recognition. It is not clear how DAMPs, particularly extracellular ATP, are regulated to modulate allograft immunity. Here we found that, following skin allotransplants, the P2X7 receptor causes ATP release from innate immune cells and that this signaling activates the NLRP3 inflammasome to release IL-18, which in turn mediates the induction of IFN-γ and the destructive Th1 response to allografts.

During organ transplant surgery or after the killing of grafted cells there is a release of several DAMPs that activate immunity in allografts (Kono and Rock, 2008; Matzinger, 2002; Oberbarnscheidt and Lakkis, 2014). In particular, extracellular ATP has been found to increase in mouse models of graft *vs.* host disease after tissue damage induced by external radiation to deplete the bone marrow compartment (Wilhelm et al., 2010). In the skin transplantation model used in the present study, syngeneic and allogeneic grafts followed the same surgical procedure but resulted in different concentrations of extracellular ATP. During allograft rejection there was a reduction in extracellular ATP, suggesting that the release of ATP in allogeneic transplants was not solely a passive consequence of tissue damage during the surgery procedure or due to immune rejection of grafted cells. ATP can be released via different active processes independently of cell death (Venereau et al., 2015) and here we demonstrate that macrophages release ATP by a mechanism dependent on the P2X7 receptor, thus reiterating the finding of an earlier recombinant cell culture study that demonstrated the role of P2X7 receptor activation in inducing ATP efflux (Pellegatti et al., 2005). Although the P2X7 channel pore is of sufficient size (1.4 nm diameter) to allow the release of ATP (~0.7 nm) (Browne et al., 2013), the electrostatic cationic profile inside the P2X7 channel could impair the direct transport of the negatively charged ATP molecule. Therefore, the P2X7 receptor may need to combine with accessory anionic channels, such as pannexin-1, to mediate the release of ATP from macrophages during allogeneic transplantation (Ma et al., 2009; Pelegrin, 2011a; Pelegrin and Surprenant, 2006; Schachter et al., 2008). However, we cannot rule out that extracellular ATP in allotransplants could also be a result of necrosis or necroptotic cell death given that the P2X7 receptor has been implicated in necrosis (Dagvadorj et al., 2015). However, in the present study, ATP release was not correlated with tissue damage, suggesting necrosis is not responsible for the elevated extracellular ATP. Recent reports have demonstrated that early innate immune processes in allografts control later adaptive rejection responses by inducing T and B cell migration and activation (Oberbarnscheidt et al., 2014). Our study suggests that extracellular ATP released by macrophages in skin allotransplants is an essential signaling system that drives the events inherent to allotransplantation and the subsequent deleterious adaptive immune rejection. However, we cannot rule out that in other transplant scenarios, extracellular ATP in allografts could also be due to other tissue-resident cells, such as myocytes or pancreatic islet cells, which have also been reported to release ATP in different pathological scenarios (Clarke et al., 2009; Kowal et al., 2015).

After we had established the role of P2X7 activation and ATP release in allogenic transplant rejection, we determined the key downstream signaling mechanisms involved and identified NLRP3 activation and IL-18 signaling as the principal allogenic mediators (Idzko et al., 2014). IL-18 is an inflammasome-dependent cytokine that potently induces a Th1 response and, unlike IL-1β, pro-IL-18 is expressed basally (Novick et al., 2013); therefore, the single step of inflammasome activation results in the release of mature IL-18. Accordingly, our study found increases in serum IL-18 in response to allograft transplantation but no changes in IL-1β.

We found that NLRP3 is the essential PRR involved in inflammasome formation in allogeneic transplant rejection and that NLRP3 dependent IL-18 maturation, not IL-1β, was necessary to stimulate T cell proliferation, IFN-γ release and the adaptive allogeneic immune response observed seven days after allogeneic transplantation. Furthermore, one of the early signs of skin rejection is epithelial hyperplasia (Lee et al., 2009), and we found that epithelial thickness decreased in allografts on both P2X7-deficient and NLRP3-deficient mice. This was further confirmed by a decrease in the Banff pathological classification for skin allografts (Cendales et al., 2008), where P2X7 or NLRP3 inflammasome deficiency reduced the severity of rejection when assessed 7 days after transplantation. IL-18 deficient mice, but not IL-1 receptor type 1 knock-out mice, presented reduced IL-12 production and T-cell alloreactivity, thus confirming previous reports where IL-18 has been found to mediate acute rejection in heart and in kidney transplantation (Affleck et al., 2001; Dudler et al., 2007; Striz et al., 2005). Deficiency or antagonism of the P2X7 receptor also resulted in increased skin allograft survival, reduced IFN-γ production, impaired T-cell alloreactivity, decreased immune cell infiltration in the transplant and reduced production of allogeneic antibodies. This suggests that a complete allograft immune rejection response depends on the P2X7 receptor signaling to the NLRP3 inflammasome via the production of IL-18 in sterile conditions, despite the fact that these do not control the early infiltration of macrophages (the present study) or the inflammatory monocytes in the allograft (Oberbarnscheidt et al., 2014).

Potential anti-inflammatory drugs have been developed using drug-like antagonists to target the P2X7 receptor (Arulkumaran et al., 2011; North and Jarvis, 2013). Clinical trials have begun on different selective P2X7 receptor antagonists, with the AstraZeneca AZD9056 compound demonstrating beneficial effects in phase IIa for Crohn's disease and inflammatory arthritis (Eser et al., 2015; Keystone et al., 2012). In the present study, we also provide evidence that pharmacological targeting of the P2X7 receptor *in vivo* delays allogeneic graft rejection and increases graft survival, which suggests that this receptor could be a therapeutic target for inducing tolerance without causing severe immunosuppression and supports previous findings that blocking purinergic signaling has a beneficial effect on lung and heart allograft survival (Liu et al., 2014; Vergani et al., 2013; 2014). P2X7 receptor expression has been associated with disease severity and has been found at higher levels in macrophages associated with coronary disease or rheumatoid arthritis (Al-Shukaili et al., 2007; Stachon et al., 2017; Zanin et al., 2015). Similarly, P2X7 receptor expression increases in the central nervous system during status epilepticus or optic nerve injury (Jimenez-Pacheco et al., 2013;

Nadal-Nicolás et al., 2016). Significantly, P2X7 receptor expression has also been found in mononuclear cells infiltrating allogeneic transplants (Vergani et al., 2013 and the present study). Furthermore, we also found an increase in P2X7 receptor expression in inflammatory blood monocytes during human liver transplantation rejection; that is, the rejection severity (measured by the increase in plasma liver enzymes) correlated with the concentration of plasma ATP. Therefore, the increase in P2X7 receptor expression in monocytes during rejection suggests a higher degree of inflammation and, according to our results, a potentially higher risk of graft rejection. In conclusion, our findings show that early ATP released by innate immune cells as a danger signal modulates the activation of the innate and adaptive immune response in allotransplants by activating the NLRP3 inflammasome and IL-18 production.

EXPERIMENTAL PROCEDURES

Human clinical samples. All samples were obtained under informed consent. This study was approved by the ethical committee of the "*Hospital Clínico Universitario Virgen de la Arrixaca*" (Murcia, Spain, with reference number PI12/02042), in accordance with the ethical guidelines of the 1975 Declaration of Helsinki. Eight liver transplant patients were subjected to progressive immunosuppressive drug withdrawal (**Table S1**). Four of these patients suffered acute rejection during the immunosuppression withdrawal process (non-tolerant patients), while the other four patients became tolerant and have been living free of immunosuppressive drugs for no less than 1 year (tolerant patients).

Mice skin transplantation. Mice were maintained in specific pathogen-free conditions at a room temperature of 22 ± 2°C, and a 12 h:12 h light/dark cycle. The mice were fed with a sterile commercial pellet diet and sterile tap water ad libitum. Skin transplantation procedure was approved by *Servicio de Sanidad Animal, Dirección General de Ganadería y Pesca, Consejería de Agricultura y Agua, Región de Murcia* (reference number C1310050305). Skin transplantation was conducted in accordance with previous protocols (Garrod and Cahalan, 2008). Transplantations were made using male 6-8 week old wild-type C57BL/6 mice or *Nlrp3*$^{-/-}$, *Casp1/11*$^{-/-}$, *P2rx7*$^{-/-}$ *Il1r1*$^{-/-}$ and *Il18*$^{-/-}$ mice (all in C57BL/6 background) as receptors (Kuida et al., 1995; Martinon et al., 2006; Solle et al., 2000). Male 6-8 week old BALB/c mice were used as donors in allogeneic transplantations, while C57BL/6 mice were used as donors in isogeneic transplantations. Analgesic and anesthetic levels were carefully monitored every 10 min during the surgical transplant procedure to ensure they were correct. After surgery, animals presenting dehydration were given saline solution. The animals' wellbeing was monitored twice per day during the first 7 days after surgery by observing their general aspect and ability to drink, feed and move normally. No animals had to be sacrificed due to any unexpected significant decrease in animal wellbeing after surgical procedure.

***In vivo* bioluminescence for extracellular ATP.** 10^6 pmeLuc cells (Morciano et al., 2017; Pellegatti et al., 2005) or 10^5 HEK293 cells transfected with pLG4.51 were inoculated under the skin graft for 1h before recording. Then D-Luciferin was inoculated intraperitoneally (150 mg/kg, 5 min). Imaging was carried out on an IVIS 100 System™ (Xenogen). Living Image® software (PerkinElmer) was used to obtain total photon counts during 15 min of the regions around the skin graft. Apyrase (4 UI) was inoculated under the skin transplant 10 min before imaging.

Skin transplant ultrasound. Skin transplants were evaluated daily using the Vevo® 3100 Imaging System (Visual Sonics Inc.), with a high frequency probe at 30Mhz. Transversal images of the transplanted area were taken. The infiltrate tissue under the skin graft was

measured from the ultrasound image and the structure of the skin layers was used to determine the survival of the graft as detailed below.

Histopathology. Syngeneic and allogeneic grafts were fixed (4% formalin, 24h), processed, paraffin-embedded and sectioned. Hematoxylin and eosin staining were used to evaluate the Banff pathological classification for skin allografts (Cendales et al., 2008). The image analysis software Axio Vision (Ver. 4.8.2, Carl Zeiss) was used to measure epidermal thickness by taking the length from the basement membrane to the stratum corneum; at least 10 measurements were taken per single 400x field in 10 fields per sample and from at least 4 different transplants. An indirect ABC-peroxidase was used to detect different immune cell populations in the graft; sections were blocked briefly (3% BSA, 20 min, 37ºC) and incubated (overnight, 4ºC) with primary antibody (1:500 for anti-CD3, Dako, 1:100 for anti-F4/80, AbD; 1:300 for CD8, Abcam; and 1:100 for FOXP3, eBioscience). Sections were examined with a Zeiss Axio Scope AX10 microscope with an AxioCamICC3 (Carl Zeiss).

Skin graft survival. Ultrasound imaging, histopathological examination and macroscopic inspection were used to generate an index to evaluate the survival of the skin graft. A graft was considered rejected when it showed the following: 1) hypoechogenic necrotic areas in dermis analyzed by ultrasound and histopathology; 2) abnormal epidermal and dermal constitution detected by ultrasound and histopathology; 3) the presence of eschar formation; and 4) independence of the graft from the surrounding skin. The Banff score was also taken into account.

ELISA. Cytokines were detected in cell supernatants and mice serum samples by ELISA (R&D, Affymetriz eBiosciences and Cloud Clone Corporation) in accordance with the manufacturer's indications.

Flow cytometry. Frozen PBMCs were thawed and dead cells were removed (Miltenyi Biotec). Live cells were incubated with Human BD FC block (BD Biosciences). Cells were stained with anti-human CD14, anti-human CD16 (BD Biosciences) and anti-human P2X7 receptor (clone L4) (Buell et al., 1998). Cells were subjected to flow cytometry analysis in a Cube 8 flow cytometer (Sysmex) The frequency of inflammatory monocytes ($CD14^{+}CD16^{++}$) and the mean fluorescent intensity of the P2X7 receptor was determined with FCS Express 5 software (DeNovo Software).

Quantitative reverse transcriptase-PCR analysis. qRT-PCR was conducted in accordance with the detailed methods described elsewhere in the literature (López-Castejón et al., 2011).

Statistical analysis. Statistics were calculated with Prism software (GraphPad). For two-group comparisons, a two-tailed unpaired *t*-test was used. Comparisons of multiple groups

were analyzed using one-way or two-way analysis of variance with Bonferroni's multiple-comparison test. The Gehan-Breslow-Wilcoxon test was used to compare differences in the transplant survival curves. Data are presented as mean ± SEM from the number of independent experiments presented in the figure legends. *p< 0.05; **p< 0.01; ***p< 0.001; *ns*, no significant difference (p> 0.05).

AUTHOR CONTRIBUTIONS

J.A.-I., M.B.-C., C.M.M. and A.B.-M. executed the experiments; F.D.V. provided the pmeLuc-HEK probe and helped with *in vivo* ATP determination; J.A.-I., M.B.-C., C.M.M., A.B.-M. and P.Pe. analyzed and interpreted the experiments; A.B.-M., B.R.-N., J.A.P., L.M.-A. and P.Pa. provided and analyzed the human clinical data; J.A.-I., C.M.M., F.D.V. and P.Pe. prepared the manuscript; P.Pe. conceived, designed, and supervised this study.

ACKNOWLEDGMENTS

We thank J. Rivers-Auty (University of Manchester, UK) for critically reading the manuscript, I. Couillin (University of Orleans, France) for the *Il1r1*$^{-/-}$, *Casp1/11*$^{-/-}$ and *Nlrp3*$^{-/-}$ mice, M. Campbell (Trinity College Dublin, Ireland) for the *Il18*$^{-/-}$ mice, the Pathology and Genomics Platforms of the Biomedical Research Institute of Murcia, and M.C. Baños and A.I. Gómez (IMIB-Arrixaca, Spain) for technical assistance with molecular and cellular biology and animal handling. J.A.-I. is supported by a Sara Borrell postdoctoral grant from the *Instituto Salud Carlos III* (CD13/00059). F.D.V. is supported by the Italian Association for Cancer Research (IG 5354), *Telethon* (GGP06070), the ERA-NET Neuron Joint Transnational Project "Nanostroke", the Italian Ministry of Health (RF-2011-02348435), the Italian Ministry of Education, University and Research (RBAP11FXBC_001) and institutional funds from the University of Ferrara. P.Pe. and F.D.V. would like to acknowledge networking support from COST Action BM-1406. Primary funding for this study was provided by the *Instituto Salud Carlos III–Fondo Europeo de Desarrollo Regional* (EMER07/049, PS09/00120 and PI13/00174 to P.Pe. and PI12/02042 to J.A.P.), Sysmex (to P.Pe.) and the European Research Council (ERC-2013-CoG 614578 to P.Pe.).

REFERENCES

Affleck, D.G., Bull, D.A., Albanil, A., Shao, Y., Brady, J., Karwande, S.V., Eichwald, E.J., Shelby, J., 2001. Interleukin-18 production following murine cardiac transplantation: correlation with histologic rejection and the induction of INF-gamma. J. Interferon Cytokine Res. 21, 1–9. doi:10.1089/107999001459105

Al-Shukaili, A., Al-Kaabi, J., Hassan, B., 2007. A Comparative Study of Interleukin-1β Production and P2x7 Expression After Atp Stimulation by Peripheral Blood Mononuclear Cells Isolated From Rheumatoid Arthritis Patients and Normal Healthy Controls. Inflammation 31, 84–90. doi:10.1007/s10753-007-9052-0

Arulkumaran, N., Unwin, R.J., Tam, F.W., 2011. A potential therapeutic role for P2X7 receptor (P2X7R) antagonists in the treatment of inflammatory diseases. Expert Opin Investig Drugs 20, 897–915. doi:10.1517/13543784.2011.578068

Baroja-Mazo, A., Martin-Sanchez, F., Gomez, A.I., Martínez, C.M., Amores-Iniesta, J., Compan, V., Barberà-Cremades, M., Yagüe, J., Ruiz-Ortiz, E., Antón, J., Buján, S., Couillin, I., Brough, D., Arróstegui, J.I., Pelegrin, P., 2014. The NLRP3 inflammasome is released as a particulate danger signal that amplifies the inflammatory response. Nat Immunol 15, 738–748. doi:10.1038/ni.2919

Bentley, T.S., Phillips, S.J., 2017. 2017 U.S. organ and tissue transplant cost estimates and discussion. Millman Research Report http://publications.milliman.com/research/health-rr/pdfs/2011-us-organ-tissue.pdf, 1–20.

Browne, L.E., Compan, V., Bragg, L., North, R.A., 2013. P2X7 receptor channels allow direct permeation of nanometer-sized dyes. J Neurosci 33, 3557–3566. doi:10.1523/JNEUROSCI.2235-12.2013

Buell, G., Chessell, I.P., Michel, A.D., Collo, G., Salazzo, M., Herren, S., Gretener, D., Grahames, C., Kaur, R., Kosco-Vilbois, M.H., Humphrey, P.P., 1998. Blockade of human P2X7 receptor function with a monoclonal antibody. Blood 92, 3521–3528.

Cassel, S.L., Sutterwala, F.S., 2010. Sterile inflammatory responses mediated by the NLRP3 inflammasome. Eur J Immunol 40, 607–611. doi:10.1002/eji.200940207

Cendales, L.C., Kanitakis, J., Schneeberger, S., Burns, C., Ruiz, P., Landin, L., Remmelink, M., Hewitt, C.W., Landgren, T., Lyons, B., Drachenberg, C.B., Solez, K., Kirk, A.D., Kleiner, D.E., Racusen, L., 2008. The Banff 2007 working classification of skin-containing composite tissue allograft pathology. Am J Transplant 8, 1396–1400. doi:10.1111/j.1600-6143.2008.02243.x

Clarke, T.C., Williams, O.J.S., Martin, P.E.M., Evans, W.H., 2009. ATP release by cardiac myocytes in a simulated ischaemia model. Eur J Pharmacol 605, 9–14. doi:10.1016/j.ejphar.2008.12.005

Critchley, W.R., Fildes, J.E., 2012. Graft rejection - endogenous or allogeneic? Immunology 136, 123–132. doi:10.1111/j.1365-2567.2012.03560.x

Dagvadorj, J., Shimada, K., Chen, S., Jones, H.D., Tumurkhuu, G., Zhang, W., Wawrowsky, K.A., Crother, T.R., Arditi, M., 2015. Lipopolysaccharide Induces Alveolar Macrophage Necrosis via CD14 and the P2X7 Receptor Leading to Interleukin-1α Release. Immunity 42, 640–653. doi:10.1016/j.immuni.2015.03.007

Di Virgilio, F., Dal Ben, D., Sarti, A.C., Giuliani, A.L., Falzoni, S., 2017. The P2X7 Receptor in Infection and Inflammation. Immunity 47, 15–31. doi:10.1016/j.immuni.2017.06.020

Donnelly-Roberts, D.L., Jarvis, M.F., 2007. Discovery of P2X7 receptor-selective antagonists offers new insights into P2X7 receptor function and indicates a role in chronic pain states. Br J Pharmacol 151, 571–579. doi:10.1038/sj.bjp.0707265

Dudler, J., Simeoni, E., Fleury, S., Li, J., Pagnotta, M., Pascual, M., Segesser, von, L.K., Vassalli, G., 2007. Gene transfer of interleukin-18-binding protein attenuates cardiac allograft rejection. Transpl. Int. 20, 460–466. doi:10.1111/j.1432-2277.2007.00457.x

Eser, A., Colombel, J.-F., Rutgeerts, P., Vermeire, S., Vogelsang, H., Braddock, M., Persson, T., Reinisch, W., 2015. Safety and Efficacy of an Oral Inhibitor of the Purinergic Receptor P2X7 in Adult Patients with Moderately to Severely Active Crohn's Disease: A Randomized Placebo-controlled, Double-blind, Phase IIa Study. Inflamm. Bowel Dis. 21, 2247–2253. doi:10.1097/MIB.0000000000000514

Ferrari, D., Pizzirani, C., Adinolfi, E., Lemoli, R.M., Curti, A., Idzko, M., Panther, E., Di Virgilio, F., 2006. The P2X7 receptor: a key player in IL-1 processing and release. J Immunol 176, 3877–3883.

Garrod, K.R., Cahalan, M.D., 2008. Murine skin transplantation. J Vis Exp e634. doi:10.3791/634

Idzko, M., Ferrari, D., Eltzschig, H.K., Eltzschig, H.K., 2014. Nucleotide signalling during inflammation. Nature 509, 310–317. doi:10.1038/nature13085
Jimenez-Pacheco, A., Mesuret, G., Sanz-Rodriguez, A., Tanaka, K., Mooney, C., Conroy, R., Miras-Portugal, M.T., Diaz-Hernandez, M., Henshall, D.C., Engel, T., 2013. Increased neocortical expression of the P2X7 receptor after status epilepticus and anticonvulsant effect of P2X7 receptor antagonist A-438079. Epilepsia 54, 1551–1561. doi:10.1111/epi.12257
Keystone, E.C., Wang, M.M., Layton, M., Hollis, S., McInnes, I.B., D1520C00001 Study Team, 2012. Clinical evaluation of the efficacy of the P2X7 purinergic receptor antagonist AZD9056 on the signs and symptoms of rheumatoid arthritis in patients with active disease despite treatment with methotrexate or sulphasalazine. Ann Rheum Dis 71, 1630–1635. doi:10.1136/annrheumdis-2011-143578
Komada, T., Usui, F., Kawashima, A., Kimura, H., Karasawa, T., Inoue, Y., Kobayashi, M., Mizushina, Y., Kasahara, T., Taniguchi, S., Muto, S., Nagata, D., Takahashi, M., 2015. Role of NLRP3 Inflammasomes for Rhabdomyolysis-induced Acute Kidney Injury. Sci Rep 5, 10901. doi:10.1038/srep10901
Kono, H., Rock, K.L., 2008. How dying cells alert the immune system to danger. Nat Rev Immunol 8, 279–289. doi:10.1038/nri2215
Kowal, J.M., Yegutkin, G.G., Novak, I., 2015. ATP release, generation and hydrolysis in exocrine pancreatic duct cells. Purinerg Signal 11, 533–550. doi:10.1007/s11302-015-9472-5
Kuida, K., Lippke, J.A., Ku, G., Harding, M.W., Livingston, D.J., Su, M.S., Flavell, R.A., 1995. Altered cytokine export and apoptosis in mice deficient in interleukin-1 beta converting enzyme. Science 267, 2000–2003.
Land, W.G., 2012. Emerging role of innate immunity in organ transplantation part II: potential of damage-associated molecular patterns to generate immunostimulatory dendritic cells. Transplant Rev (Orlando) 26, 73–87. doi:10.1016/j.trre.2011.02.003
Latz, E., Xiao, T.S., Stutz, A., 2013. Activation and regulation of the inflammasomes. Nat Rev Immunol 13, 397–411. doi:10.1038/nri3452
Lee, P., Lee, D.-J., Chan, C., Chen, S.-W., Ch'en, I., Jamora, C., 2009. Dynamic expression of epidermal caspase 8 simulates a wound healing response. Nature 458, 519–523. doi:10.1038/nature07687
Liu, K., Vergani, A., Zhao, P., Ben Nasr, M., Wu, X., Iken, K., Jiang, D., Su, X., Fotino, C., Fiorina, P., Visner, G.A., 2014. Inhibition of the purinergic pathway prolongs mouse lung allograft survival. Am J Respir Cell Mol Biol 51, 300–310. doi:10.1165/rcmb.2013-0362OC
López-Castejón, G., Baroja-Mazo, A., Pelegrin, P., 2011. Novel macrophage polarization model: from gene expression to identification of new anti-inflammatory molecules. Cell Mol Life Sci 68, 3095–3107. doi:10.1007/s00018-010-0609-y
Ma, W., Ma, W., Hui, H., Hui, H., Pelegrin, P., Pelegrin, P., Surprenant, A., Surprenant, A., 2009. Pharmacological characterization of pannexin-1 currents expressed in mammalian cells. Journal of Pharmacology and Experimental Therapeutics 328, 409–418. doi:10.1124/jpet.108.146365
Martinon, F., Pétrilli, V., Mayor, A., Tardivel, A., Tschopp, J., 2006. Gout-associated uric acid crystals activate the NALP3 inflammasome. Nature 440, 237–241. doi:10.1038/nature04516
Matzinger, P., 2002. The Danger Model: A Renewed Sense of Self. Science 296, 301–305. doi:10.1126/science.1071059
Miao, E.A., Rajan, J.V., Aderem, A., 2011. Caspase-1-induced pyroptotic cell death. Immunol Rev 243, 206–214. doi:10.1111/j.1600-065X.2011.01044.x
Morciano, G., Sarti, A.C., Marchi, S., Missiroli, S., Falzoni, S., Raffaghello, L., Pistoia, V., Giorgi, C., Di Virgilio, F., Pinton, P., 2017. Use of luciferase probes to measure ATP in living cells and animals. Nat Protoc 12, 1542–1562. doi:10.1038/nprot.2017.052
Nadal-Nicolás, F.M., Galindo-Romero, C., Valiente-Soriano, F.J., Barberà-Cremades, M., deTorre-Minguela, C., Salinas-Navarro, M., Pelegrin, P., Agudo-Barriuso, M., 2016. Involvement of P2X7 receptor in neuronal degeneration triggered by traumatic injury. Sci Rep 6, 38499. doi:10.1038/srep38499
North, R.A., Jarvis, M.F., 2013. P2X receptors as drug targets. Mol Pharmacol 83, 759–769. doi:10.1124/mol.112.083758
Novick, D., Kim, S., Kaplanski, G., Dinarello, C.A., 2013. Interleukin-18, more than a Th1

cytokine. Semin Immunol 25, 439–448. doi:10.1016/j.smim.2013.10.014
Oberbarnscheidt, M.H., Lakkis, F.G., 2014. Innate allorecognition. Immunol Rev 258, 145–149. doi:10.1111/imr.12153
Oberbarnscheidt, M.H., Zeng, Q., Li, Q., Dai, H., Williams, A.L., Shlomchik, W.D., Rothstein, D.M., Lakkis, F.G., 2014. Non-self recognition by monocytes initiates allograft rejection. J Clin Invest 124, 3579–3589. doi:10.1172/JCI74370
Pelegrin, P., 2011a. Many ways to dilate the P2X7 receptor pore. Br J Pharmacol 163, 908–911. doi:10.1111/j.1476-5381.2011.01325.x
Pelegrin, P., 2011b. Inflammasome Activation by Danger Signals, in: The Inflammasomes. Springer Basel, Basel, pp. 101–121. doi:10.1007/978-3-0348-0148-5_7
Pelegrin, P., Surprenant, A., 2006. Pannexin-1 mediates large pore formation and interleukin-1beta release by the ATP-gated P2X7 receptor. EMBO J 25, 5071–5082. doi:10.1038/sj.emboj.7601378
Pellegatti, P., Falzoni, S., Pinton, P., Rizzuto, R., Di Virgilio, F., 2005. A novel recombinant plasma membrane-targeted luciferase reveals a new pathway for ATP secretion. Mol Biol Cell 16, 3659–3665. doi:10.1091/mbc.E05-03-0222
Schachter, J., Motta, A.P., de Souza Zamorano, A., da Silva-Souza, H.A., Guimaraes, M.Z.P., Persechini, P.M., 2008. ATP-induced P2X7-associated uptake of large molecules involves distinct mechanisms for cations and anions in macrophages. J Cell Sci 121, 3261–3270. doi:10.1242/jcs.029991
Schroder, K., Tschopp, J., 2010. The Inflammasomes. Cell 140, 821–832. doi:10.1016/j.cell.2010.01.040
Solle, M., Labasi, J., Perregaux, D.G., Stam, E., Petrushova, N., Koller, B.H., Griffiths, R.J., Gabel, C.A., 2000. Altered Cytokine Production in Mice Lacking P2X7 Receptors. J Biol Chem 276, 125–132. doi:10.1074/jbc.M006781200
Stachon, P., Heidenreich, A., Merz, J., Hilgendorf, I., Wolf, D., Willecke, F., Garlen, von, S., Albrecht, P., Härdtner, C., Ehrat, N., Hoppe, N., Reinöhl, J., Zur Mühlen, von, C., Bode, C., Idzko, M., Zirlik, A., 2017. P2X7 Deficiency Blocks Lesional Inflammasome Activity and Ameliorates Atherosclerosis in Mice. Circulation. doi:10.1161/CIRCULATIONAHA.117.027400
Striz, I., Eliska, K., Eva, H., Jiri, L., Katerina, P., Marcela, J., Alena, L., Radka, B., Sarka, V., Antonij, S., Stefan, V., 2005. Interleukin 18 (IL-18) upregulation in acute rejection of kidney allograft. Immunology Letters 99, 30–35. doi:10.1016/j.imlet.2005.01.010
Su, C.A., Iida, S., Abe, T., Fairchild, R.L., 2014. Endogenous memory CD8 T cells directly mediate cardiac allograft rejection. Am J Transplant 14, 568–579. doi:10.1111/ajt.12605
Venereau, E., Ceriotti, C., Bianchi, M.E., 2015. DAMPs from Cell Death to New Life. Front Immun 6, 422. doi:10.3389/fimmu.2015.00422
Vergani, A., Tezza, S., D'Addio, F., Fotino, C., Liu, K., Niewczas, M., Bassi, R., Molano, R.D., Kleffel, S., Petrelli, A., Soleti, A., Ammirati, E., Frigerio, M., Visner, G., Grassi, F., Ferrero, M.E., Corradi, D., Abdi, R., Ricordi, C., Sayegh, M.H., Pileggi, A., Fiorina, P., 2013. Long-term heart transplant survival by targeting the ionotropic purinergic receptor P2X7. Circulation 127, 463–475. doi:10.1161/CIRCULATIONAHA.112.123653
Vergani, A., Tezza, S., Fotino, C., Visner, G., Pileggi, A., Chandraker, A., Fiorina, P., 2014. The purinergic system in allotransplantation. Am J Transplant 14, 507–514. doi:10.1111/ajt.12567
Wilhelm, K., Ganesan, J., Müller, T., Dürr, C., Grimm, M., Beilhack, A., Krempl, C.D., Sorichter, S., Gerlach, U.V., Jüttner, E., Zerweck, A., Gärtner, F., Pellegatti, P., Di Virgilio, F., Ferrari, D., Kambham, N., Fisch, P., Finke, J., Idzko, M., Zeiser, R., 2010. Graft-versus-host disease is enhanced by extracellular ATP activating P2X7R. Nat Med 16, 1434–1438. doi:10.1038/nm.2242
Zanin, R.F., Bergamin, L.S., Morrone, F.B., Coutinho-Silva, R., De Souza Wyse, A.T., Battastini, A.M.O., 2015. Pathological concentrations of homocysteine increases IL-1β production in macrophages in a P2X7, NF-κB, and erk-dependent manner. Purinerg Signal. doi:10.1007/s11302-015-9464-5
Zecher, D., Van Rooijen, N., Rothstein, D.M., Shlomchik, W.D., Lakkis, F.G., 2009. An innate response to allogeneic nonself mediated by monocytes. J Immunol 183, 7810–7816. doi:10.4049/jimmunol.0902194

MAIN FIGURE TITLES AND LEGENDS

Figure 1. Allogeneic transplants are associated with extracellular ATP. (**A**) Representative images of extracellular ATP 3 days after syngeneic or allogeneic skin transplantation, using C57BL/6 as recipient and C57BL/6 (syngeneic) or BALB/c (allogeneic) skin as donor. (**B**) Quantification of graft-associated bioluminescence as the average radiance (p/s/cm^2/sr) at day 3 after transplantation (*n*= 8). (**C**) Extracellular ATP quantification at 3, 7 and 14 days after syngeneic or allogeneic transplantation (*n*= 7−10). (**D**) Representative images of hematoxylin and eosin stained grafts; arrows denote tissue necrosis and the detachment of epidermal layer; scale bar 50 µm. (**E**) CD3$^+$ cells 3 or 7 days after transplantation (*n*= 12−18 fields of view from 3-4 transplants). (**F**) Relative gene expression for the indicated genes in grafts 3 or 7 days after transplantation (*n*= 4-5). (**G**) IFN-γ ELISA produced by axillar lymph node lymphocytes collected 7 days after syngeneic or allogeneic transplantation and subjected to mixed lymphocytic reaction with allogeneic splenocytes (*n*= 3-6). *t*-Student for **B** and ANOVA with Bonferroni's post-test for **E**-**G**. For **B,C,E-G** data are represented as mean ± SEM. See also Figure S1.

Figure 2. Allografts induce ATP release via P2X7 receptor in antigen-presenting cells. (**A**) Extracellular ATP associated with allografts 3 days after transplantation, using C57BL/6 wild-type or *P2rx7*$^{-/-}$ as recipient and BALB/c skin as donor. Left, representative mouse per group. Right, average radiance (p/s/cm^2/sr) of *n*= 5−8 transplants. (**B**) Extracellular ATP associated with allografts 3 days after transplantation in wild-type mice treated with vehicle or A438079 (100 µmol/kg). Left, representative mouse per group. Right, p/s/cm^2/sr of *n*= 5−6 transplants. (**C**,**D**) ATP release from C57BL/6 bone marrow-derived macrophages (BMDM) incubated for 2 h with C57BL/6 or Balb/c skin (n =4) (**C**) or incubated for 30 min in the absence or presence of ovalbumin (OVA, 10 mg/ml) and A438079 (25 µM) (n =3). (**E**) Yo-Pro uptake kinetic in BMDMs treated or not for 2 h with OVA (10 mg/ml) or LPS (1 µg/ml) and then stimulated as indicated by an arrow with ATP (3 mM) in the presence or absence of A438079 (25 µM) (n =6). (**F**) Extracellular ATP associated to allografts 3 days after transplantation in *P2rx7*$^{-/-}$ mice treated with 10^6 wild-type (*P2rx7*$^{+/+}$) or *P2rx7*$^{-/-}$ BMDM applied under the skin graft during the surgical procedure. For **A**,**B**,**F**: Left, representative mouse per group. Right, p/s/cm^2/sr of *n*= 5−6 transplants. *t*-Student for **A,B,F;** ANOVA with Bonferroni's post-test for **C**,**D** or Tukey post-test for the slopes represented in **E**. Data are represented as mean ± SEM. See also Figure S2.

Figure 3. P2X7 receptor blockage reduces allograft rejection. (**A**) Representative images of hematoxylin and eosin stained allogeneic skin grafts using C57BL/6 wild-type or *P2rx7*$^{-/-}$ as recipient and BALB/c skin as donor; scale bar 50 µm. (**B**) Epidermal thickness at 3 days after transplantation. A438079 i.p. injected (100 µmol/kg/day) (*n*= 19−71 measurements from 3-4 transplants). (**C**) CD3$^+$ or F4/80$^+$cells 7 days after transplantation (*n*= 6−26 fields of view from

3-4 transplants). (**D**) IFN-γ in serum 7 days after transplantation (*n*= 3-5). (**E**) IFN-γ ELISA produced by axillar lymph node lymphocytes collected 7 days after transplantation and subjected to mixed lymphocytic reaction (MLR) with allogeneic splenocytes (*n*= 3-7). (**F,G**) Measurement of transplanted skin by ultrasound (**F**) or skin transplant survival (**G**) (*n*= 6−11 transplants). (**H**) Activity of plasma liver enzymes in human serum and mean fluorescence intensity for P2X7 receptor surface expression in inflammatory monocytes ($CD14^{+}CD16^{++}$) from liver-transplanted patients (tolerant or non-tolerant) during immunosuppression and after immunosuppression withdrawal (rejection) (*n*= 4 patients/group). (**I**) Correlation between the fold change of plasma ATP concentration and liver enzymes during immunosuppression and after immunosuppression withdrawal in the 4 non-tolerant patients. One-way ANOVA with Bonferroni's post-test for **B-E**, two-way ANOVA with Bonferroni's post-test for **F,H** (*differences between allogeneic and isogeneic; §differences between allogeneic and allogeneic+A438079; *ns*, no significant difference between isogeneic and allogeneic+A438079) and Gehan-Breslow-Wilcoxon test for **G**. For **B-F,H** data are represented as mean ± SEM. See also Figure S3, Figure S4 and Table S1.

Figure 4. The NLRP3 inflammasome is not involved in ATP release in allografts but is activated in allografts. (**A**) Extracellular ATP associated with allografts 3 days after transplantation in wild-type (*Nlrp3*$^{+/+}$) or *Nlrp3*$^{-/-}$ mice. Left, luciferase signal representing extracellular ATP in one representative mouse per group. Right, average radiance (p/s/cm^2/sr) of *n*= 7−8 transplants. **(B)** Extracellular ATP associated with allografts 3 days after transplantation in wild-type (*Casp1/11*$^{+/+}$) or *Casp1/11*$^{-/-}$ mice. Left, luciferase signal representing extracellular ATP in one representative mouse per group. Right, average radiance (p/s/cm^2/sr) of *n*= 3−4 transplants. (**C**) Relative gene expression for the indicated genes in grafts 3 days after transplantation, using C57BL/6 as recipient and C57BL/6 (syngeneic) or BALB/c (allogeneic) skin as donor. A438079 i.p. injected (100 µmol/kg/day) (*n*= 5−6). Gene expression of healthy skin is presented with a dashed line. (**D**) IL-18 ELISA in serum 3 days after transplantation (*n*= 3−5). *ns*, no significant difference (p> 0.05); *t*-Student for **A**,**B**; ANOVA with Bonferroni's post-test for **C**,**D**. Data are represented as mean ± SEM.

Figure 5. Inflammasome is upregulated during graft rejection. (**A**) *Casp1* gene expression in grafts (*n*= 3−6). (**B,C**) Relative gene expression for *Nlrp3* (**B**), *Il1b* and *Il18* (**C**) in grafts (*n*= 3-6). ANOVA with Bonferroni's post-test for **A**-**C**, and using C57BL/6 wild-type, *Nlrp3*$^{-/-}$ or *Casp1/11*$^{-/-}$ as recipient and C57BL/6 (syngeneic) or BALB/c (allogeneic) skin as donor. WT: Wild-type. Data are represented as mean ± SEM.

Figure 6. NLRP3 inflammasome deficiency reduces allogeneic immune response. (**A**) Representative images of hematoxylin and eosin stained skin grafts, using C57BL/6 wild-

type, *Nlrp3*$^{-/-}$ or *Casp1/11*$^{-/-}$ as recipient and BALB/c skin as donor; scale bar 50 μm. (**B**) Epidermal thickness at 3 days after transplantation (*n*= 20−70 measurements from 3-4 transplants). (**C**) IL-18 ELISA in serum at 3 days post-transplantation (*n*= 4−6). (**D**) CD3^{+} or F4/80^{+}cells 7 days after transplantation (*n*= 6−20 fields of view from 3-4 transplants). (**E,F**) IFN-γ relative gene expression (**E**) or serum concentration (**F**) 7 days after transplantation (*n*= 3−4, **E**; *n*= 3-8, **F**). (**G**) IFN-γ ELISA produced by axillar lymph node lymphocytes collected 7 days after transplantation and subjected to mixed lymphocytic reaction (MLR) with allogeneic splenocytes (*n*= 4-7). For **F**,**G** each circle represents an individual mouse. ANOVA with Bonferroni's post-test for **B**-**G**. For **B-G** data are represented as mean ± SEM. See also Figure S5.

Figure 7. IL-18 mediates inflammasome alloimmune response. (**A**) IL-18 binding protein (IL-18BP) (left) and the ratio of IL-18/IL-18BP (right) in serum 7 days after transplantation (*n*= 4-5) using C57BL/6 as recipient and C57BL/6 (syngeneic) or BALB/c (allogeneic) skin as donor. (**B**) Relative gene expression for *Il12b* in grafts 3 or 7 days after transplantation using C57BL/6 wild-type or *Il18*$^{-/-}$ as recipient and BALB/c skin as donor (*n*= 3-4). (**C**) IFN-γ in serum 7 days after transplantation (*n*= 3-4). (**D**) IFN-γ ELISA produced by axillar lymph node lymphocytes collected 7 days after transplantation and subjected to mixed lymphocytic reaction (MLR) with allogeneic splenocytes (*n*= 4). (**E**) Representative images of hematoxylin and eosin stained skin grafts, using C57BL/6 wild-type or *Il18*$^{-/-}$ as recipient and BALB/c skin as donor; scale bar 50 μm. (**F**) F4/80^{+}, CD3^{+}, CD8^{+} or FOXP3^{+} cells 7 days after transplantation (*n*= 24-51 fields of view from 3 transplants). For **C**,**D** each circle represents an individual mouse. *t*-Student for **A-D,F**. For **A-D,F** data are represented as mean ± SEM. See also Figure S6.

Figure 1

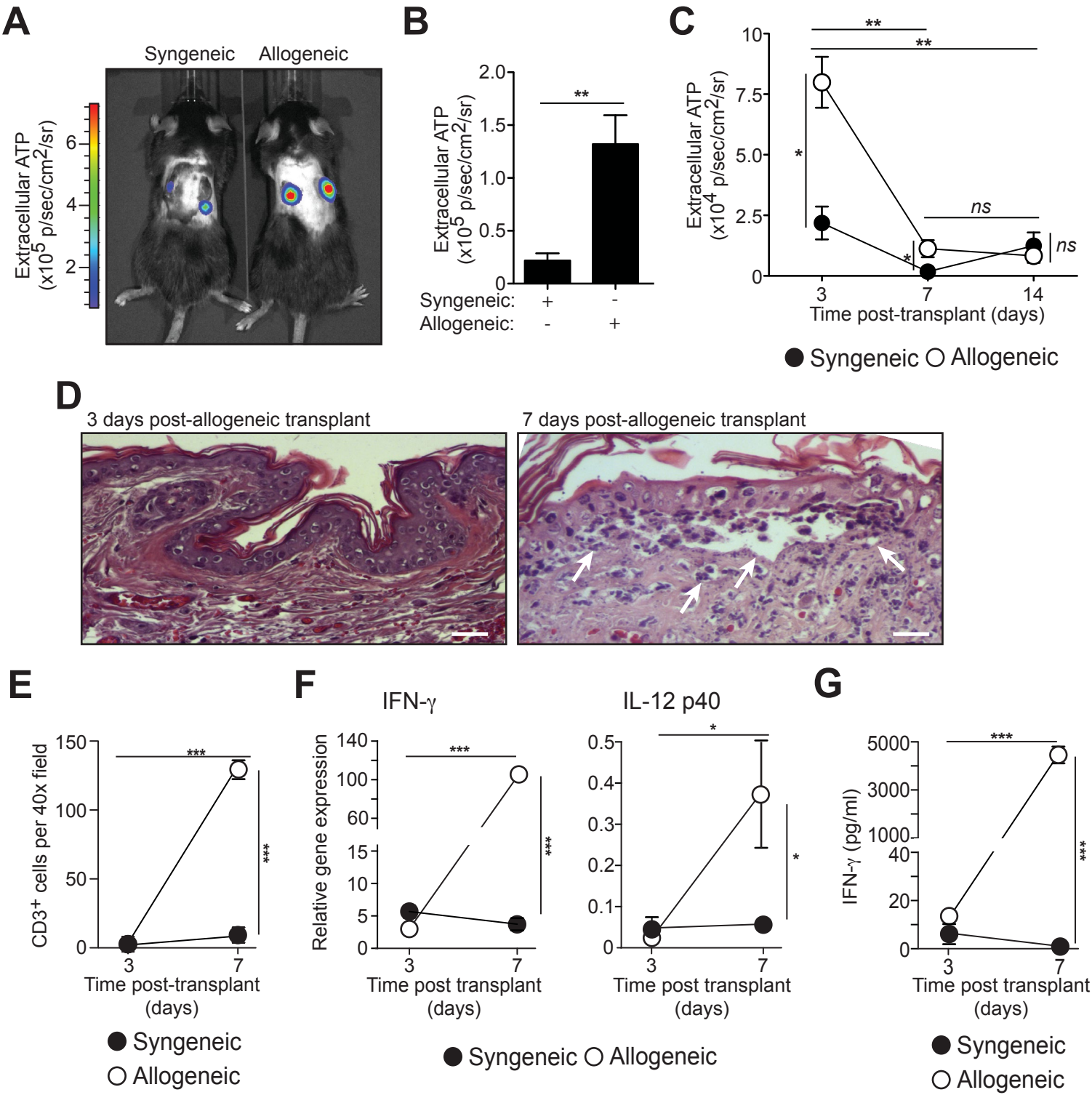
A
Syngeneic
Allogeneic
Extracellular ATP (x10^5 p/sec/cm^2/sr)
B
Extracellular ATP (x10^5 p/sec/cm^2/sr)
Syngeneic: + -
Allogeneic: - +
C
Extracellular ATP (x10^4 p/sec/cm^2/sr)
ns
Time post-transplant (days)
Syngeneic Allogeneic
D
3 days post-allogeneic transplant
7 days post-allogeneic transplant
E
CD3+ cells per 40x field
Time post-transplant (days)
Syngeneic
Allogeneic
F
IFN-γ
IL-12 p40
Relative gene expression
Time post transplant (days)
Syngeneic Allogeneic
G
IFN-γ (pg/ml)
Time post transplant (days)
Syngeneic
Allogeneic

Figure 2

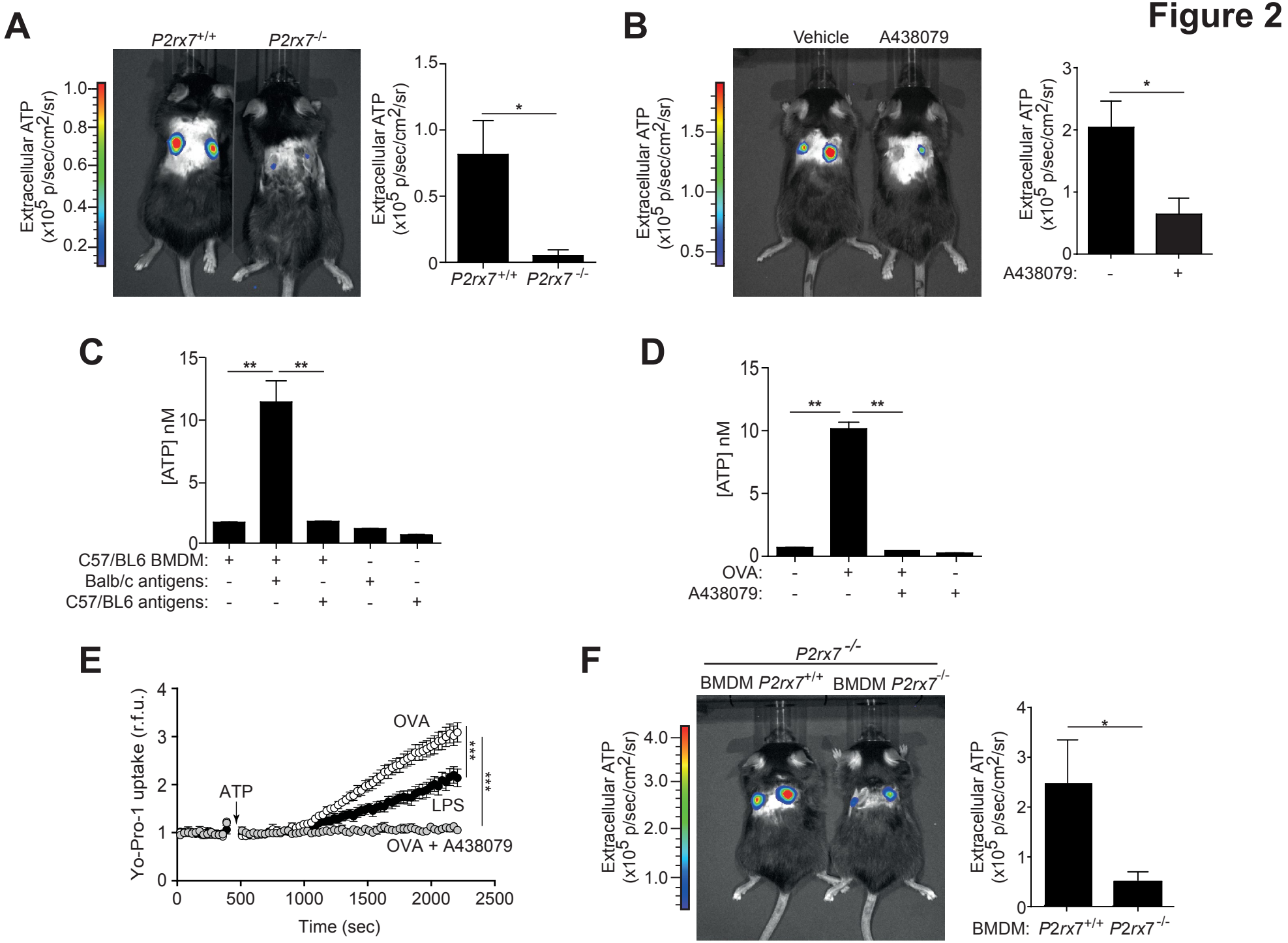
A
P2rx7+/+
P2rx7-/-
Extracellular ATP (x10^5 p/sec/cm^2/sr)
1.0
0.8
0.6
0.4
0.2
1.5
1.0
0.5
0
*
P2rx7+/+
P2rx7 -/-
B
Vehicle
A438079
Extracellular ATP (x10^5 p/sec/cm^2/sr)
1.5
1.0
0.5
3
2
1
0
*
A438079: - +
C
[ATP] nM
15
10
5
0
**
**
C57/BL6 BMDM: + + + - -
Balb/c antigens: - + - + -
C57/BL6 antigens: - - + - +
D
[ATP] nM
15
10
5
0
**
**
OVA: - + + -
A438079: - - + +
E
Yo-Pro-1 uptake (r.f.u.)
4
3
2
1
0
ATP
OVA
LPS
OVA + A438079
***
***
0
500
1000
1500
2000
2500
Time (sec)
F
P2rx7 -/-
BMDM P2rx7+/+
BMDM P2rx7-/-
Extracellular ATP (x10^5 p/sec/cm^2/sr)
4.0
3.0
2.0
1.0
4
3
2
1
0
*
BMDM: P2rx7+/+ P2rx7 -/-

Figure 3

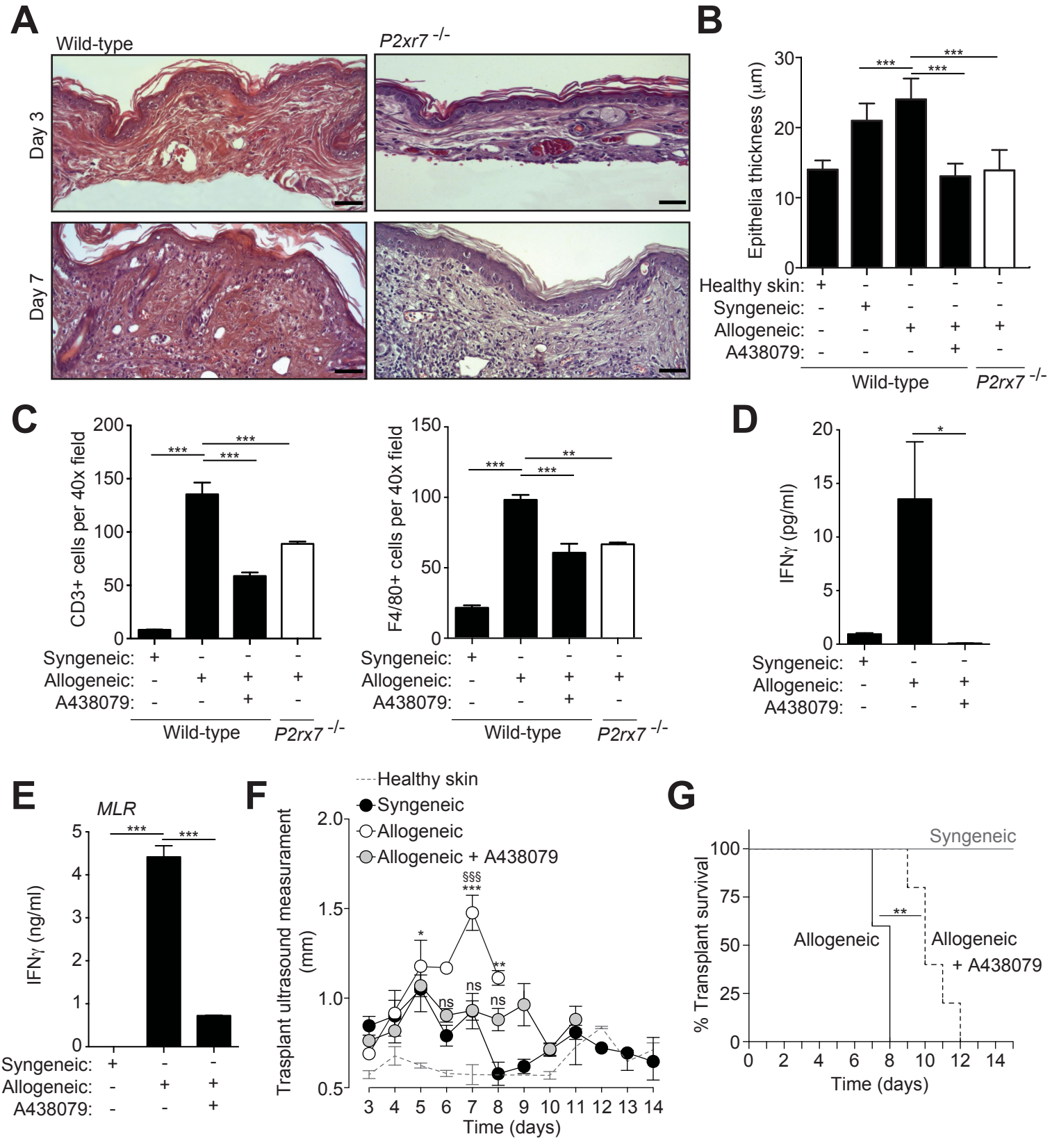
A
Wild-type
P2xr7 -/-
Day 3
Day 7
B
Epithelia thickness (µm)
Healthy skin:
Syngeneic:
Allogeneic:
A438079:
Wild-type
P2rx7 -/-
C
CD3+ cells per 40x field
F4/80+ cells per 40x field
Syngeneic:
Allogeneic:
A438079:
Wild-type
P2rx7 -/-
D
IFNγ (pg/ml)
Syngeneic:
Allogeneic:
A438079:
E
MLR
IFNγ (ng/ml)
Syngeneic:
Allogeneic:
A438079:
F
Healthy skin
Syngeneic
Allogeneic
Allogeneic + A438079
Trasplant ultrasound measurament (mm)
Time (days)
G
Syngeneic
Allogeneic
Allogeneic + A438079
% Transplant survival
Time (days)

Figure 4

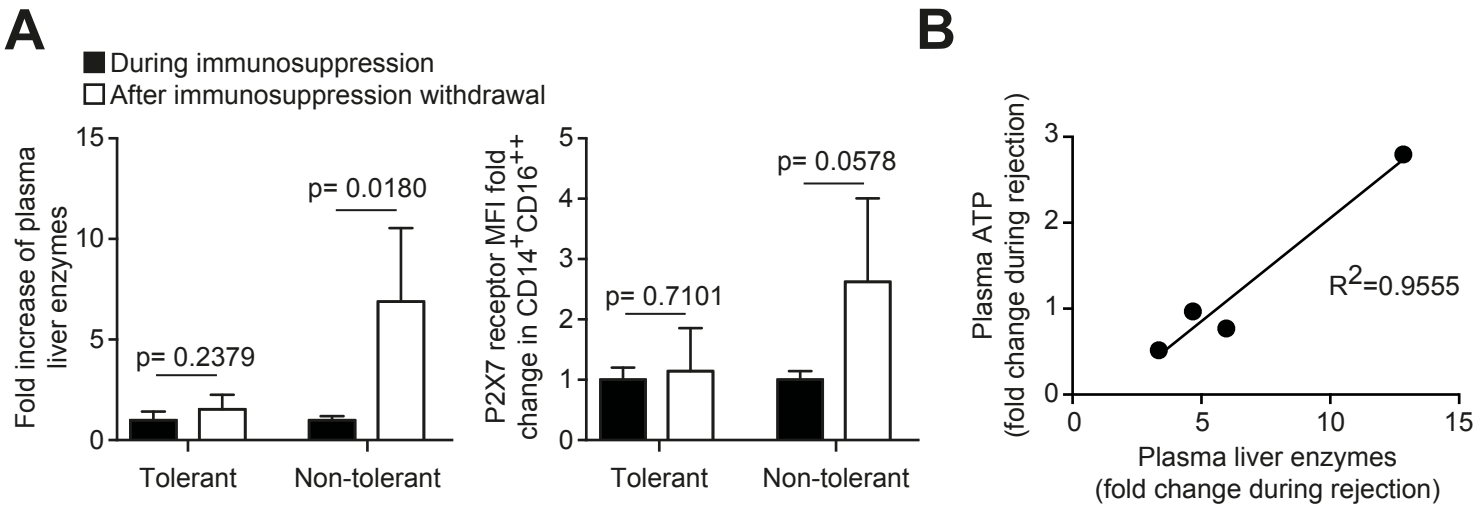
A
During immunosuppression
After immunosuppression withdrawal
Fold increase of plasma liver enzymes
15
10
5
0
p= 0.2379
p= 0.0180
Tolerant
Non-tolerant
P2X7 receptor MFI fold change in CD14+CD16++
5
4
3
2
1
0
p= 0.7101
p= 0.0578
Tolerant
Non-tolerant
B
Plasma ATP (fold change during rejection)
3
2
1
0
0
5
10
15
R2=0.9555
Plasma liver enzymes (fold change during rejection)

Figure 5

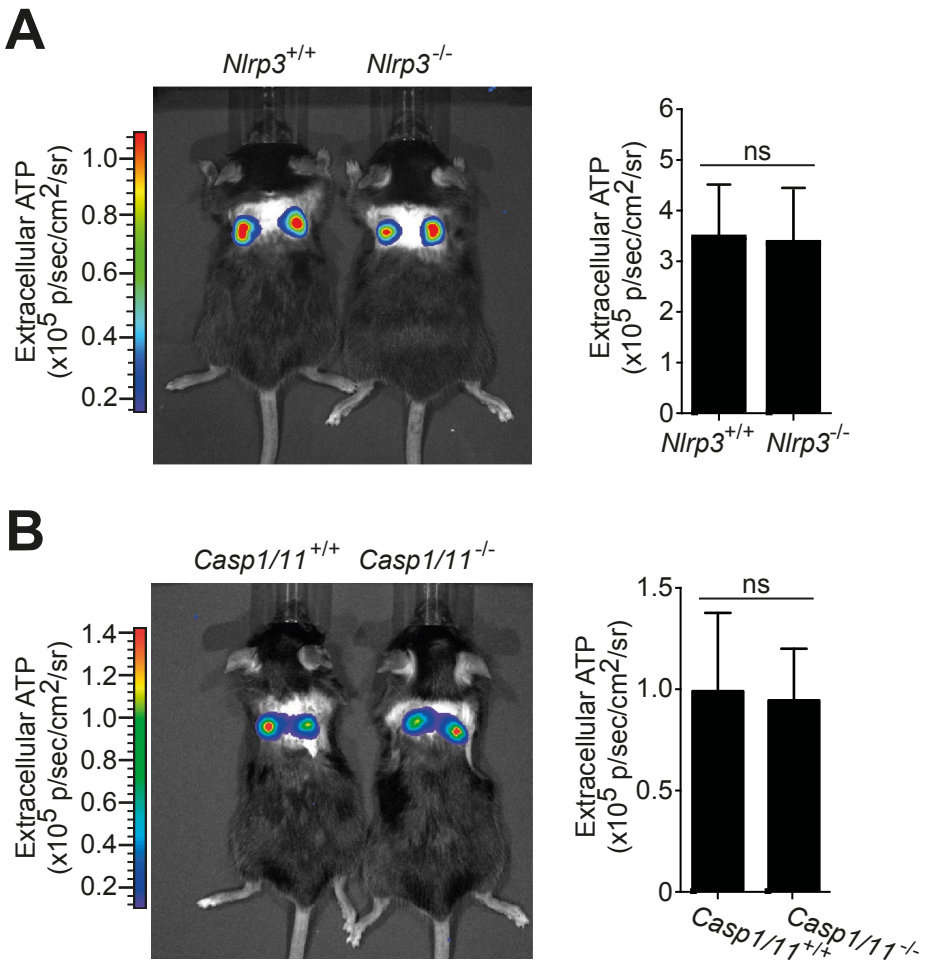
A
Nlrp3+/+
Nlrp3-/-
Extracellular ATP (x10^5 p/sec/cm2/sr)
ns
B
Casp1/11+/+
Casp1/11-/-
C
Nlrp3
Casp1
Il1b
Il18
Relative gene expression
Syngeneic:
Allogeneic:
A438079:
D
IL-18 (pg/ml)

Figure 6

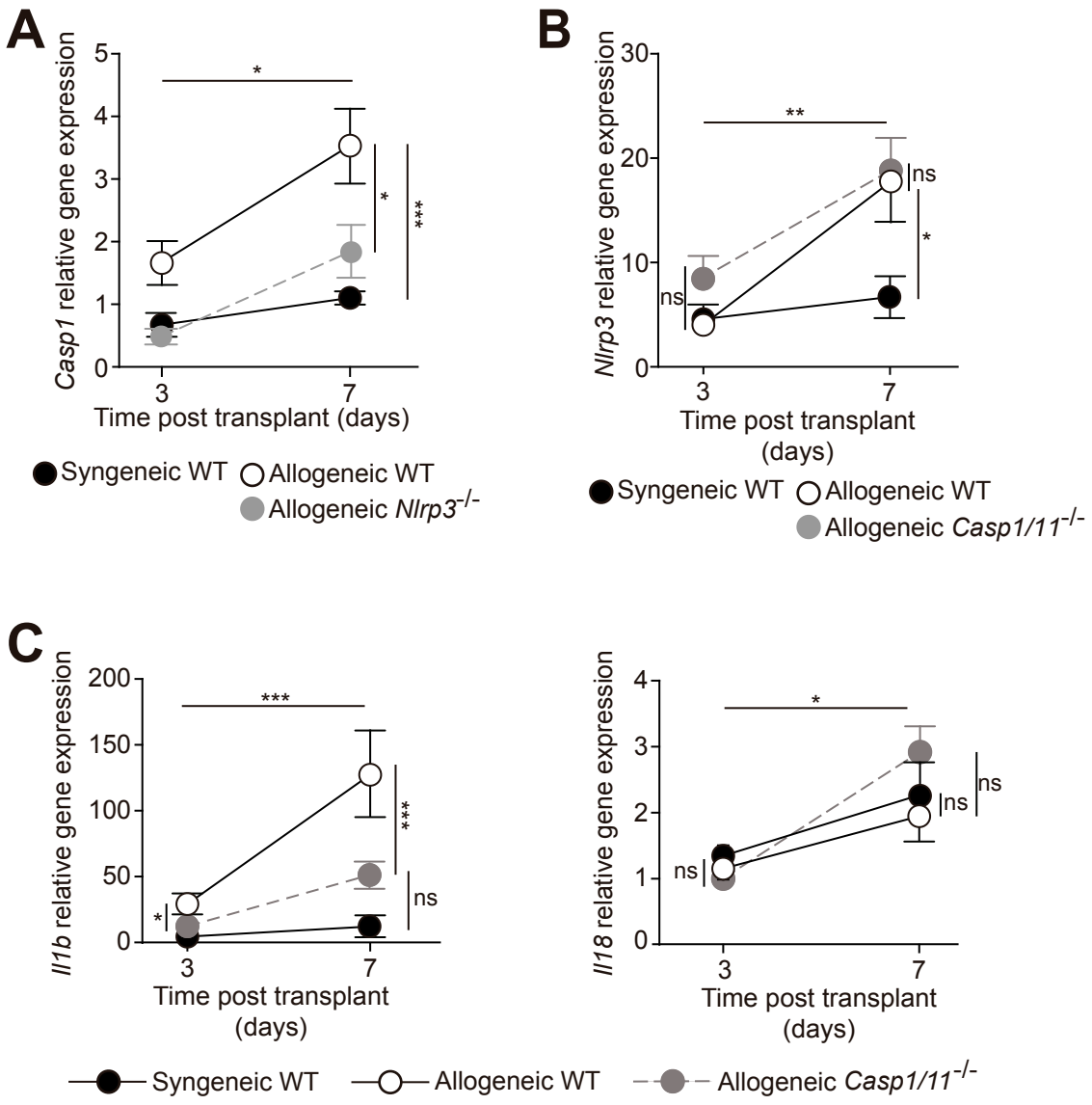
A
Casp1 relative gene expression
Time post transplant (days)
Syngeneic WT
Allogeneic WT
Allogeneic Nlrp3-/-
B
Nlrp3 relative gene expression
Time post transplant (days)
Syngeneic WT
Allogeneic WT
Allogeneic Casp1/11-/-
C
Il1b relative gene expression
Il18 relative gene expression
Time post transplant (days)
Syngeneic WT
Allogeneic WT
Allogeneic Casp1/11-/-

Figure 7

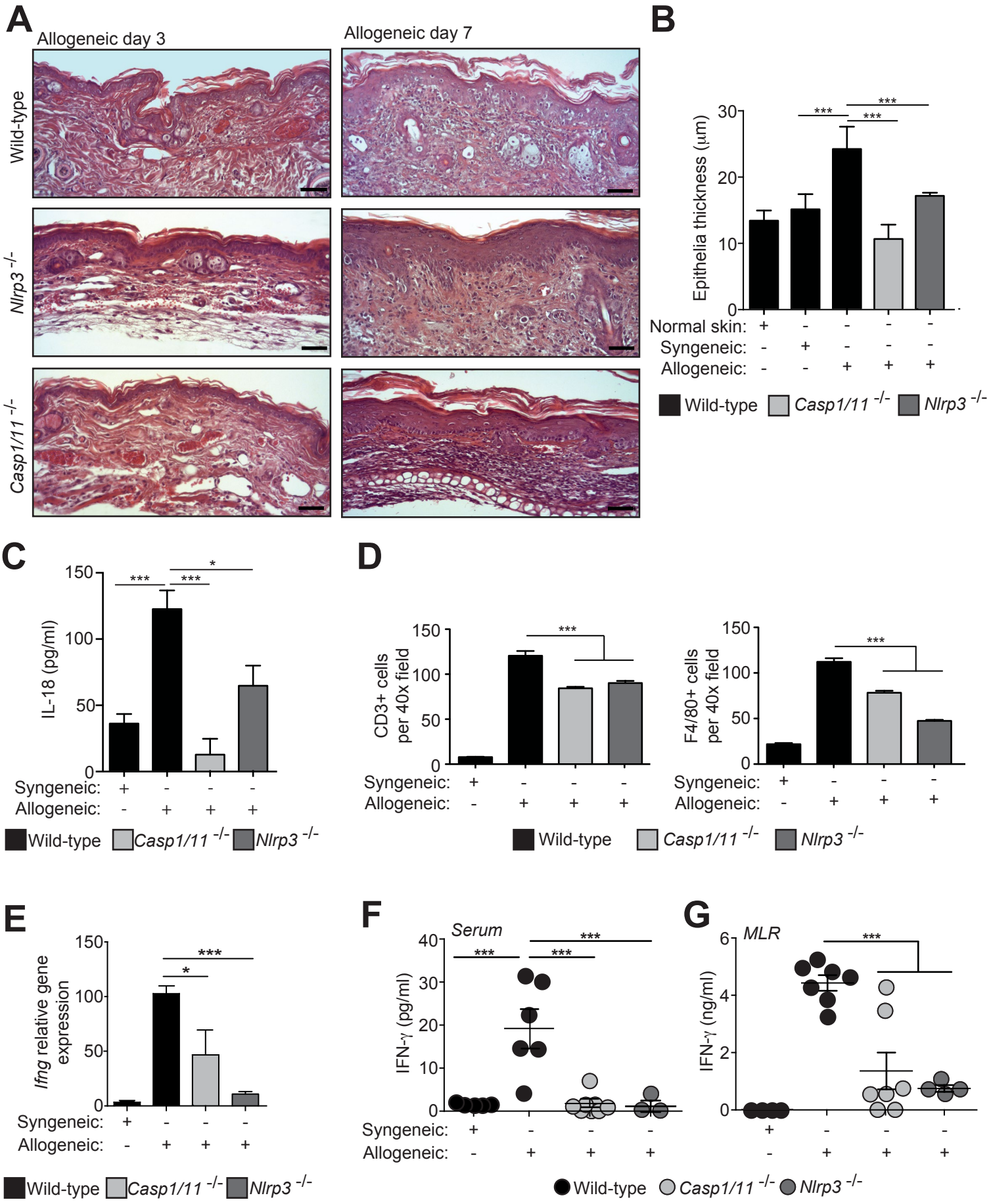
A
Allogeneic day 3
Allogeneic day 7
Wild-type
Nlrp3 -/-
Casp1/11 -/-
B
Epithelia thickness (μm)
Normal skin:
Syngeneic:
Allogeneic:
Wild-type
Casp1/11 -/-
Nlrp3 -/-
C
IL-18 (pg/ml)
Syngeneic:
Allogeneic:
Wild-type
Casp1/11 -/-
Nlrp3 -/-
D
CD3+ cells per 40x field
F4/80+ cells per 40x field
Syngeneic:
Allogeneic:
Wild-type
Casp1/11 -/-
Nlrp3 -/-
E
Ifng relative gene expression
Syngeneic:
Allogeneic:
Wild-type
Casp1/11 -/-
Nlrp3 -/-
F
Serum
IFN-γ (pg/ml)
Syngeneic:
Allogeneic:
G
MLR
IFN-γ (ng/ml)
Wild-type
Casp1/11 -/-
Nlrp3 -/-

Figure 8

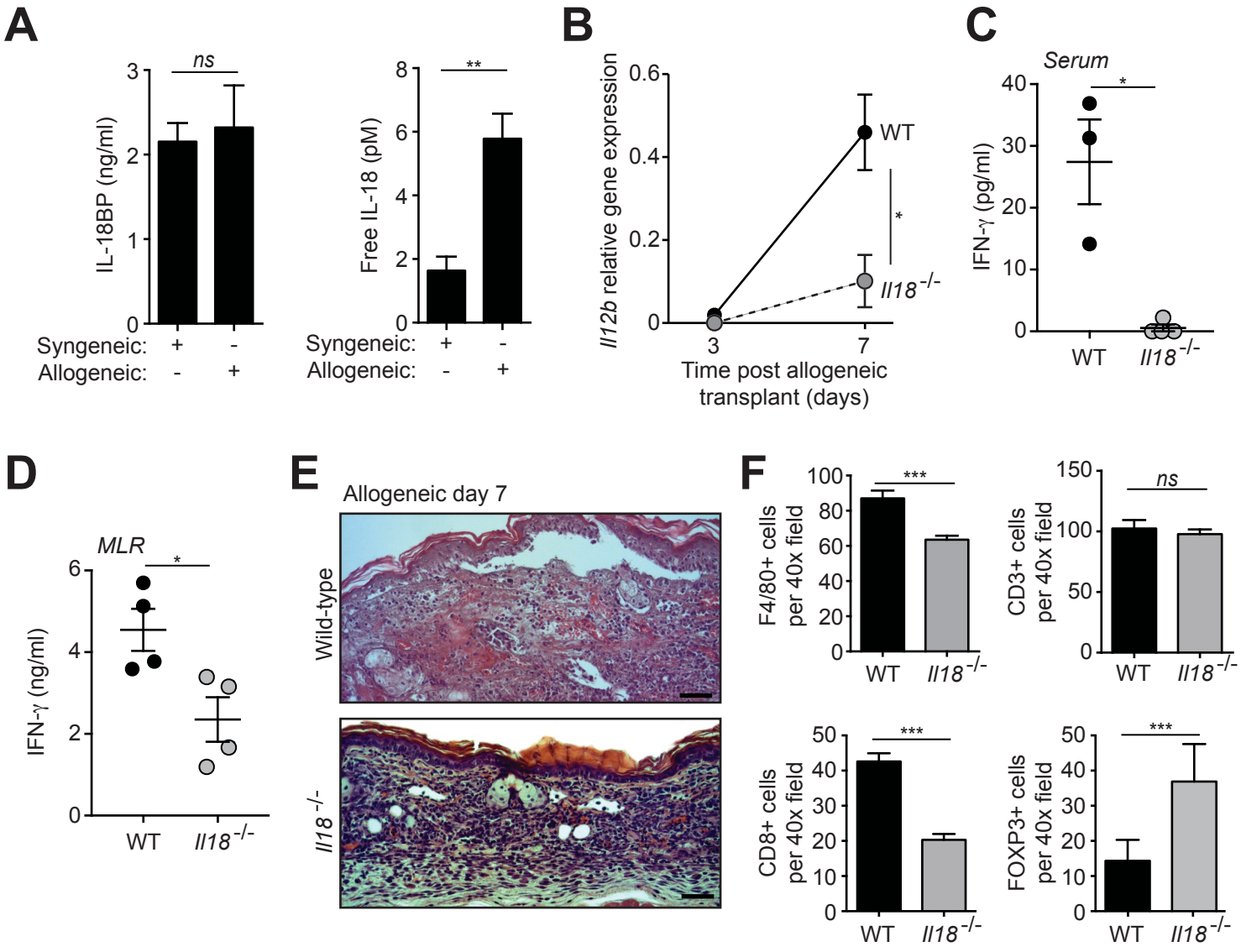
A
ns
IL-18BP (ng/ml)
Syngeneic:
Allogeneic:
**
Free IL-18 (pM)
B
Il12b relative gene expression
WT
Il18-/-
Time post allogeneic transplant (days)
C
Serum
IFN-γ (pg/ml)
D
MLR
IFN-γ (ng/ml)
E
Allogeneic day 7
Wild-type
Il18-/-
F
F4/80+ cells per 40x field
CD3+ cells per 40x field
CD8+ cells per 40x field
FOXP3+ cells per 40x field